https://doi.org/10.33472/AFJBS.6.4.2024.578-605

African Journal of Biological Sciences

Research Paper Open Access

Phosphorylated α- synculein and Autophagy in The Retina of Rotenone- Induced Rat Model of Parkinson's Disease

Rasha Abd Elrahman, Amany Shams, Mona El-Shahat, Shata Fekry E, Samira Lotfy Abd-Elhady

Corresponding author: Rasha Abd Elrahman

01002723371

Rashaeissa2016@gmail.com

Article History

Volume 6,Issue 4, Feb 2024

Received:17 Feb 2024

Accepted : 01 Mar 2024

doi:10.33472/AFJBS.6.4.2024.578-605

ABSTRACT:

Phosphorylated α-Syn is a potential biomarker of Parkinson's disease (PD). Autophagy is an internal breakdown process that removes proteins and/or ageing, damaged organelles caused by folding mistakes. This study was designed to assess the possible role of autophagy in pathogenesis of PD in the retina. PD model was induced by daily intraperitoneal injection of rotenone (2.5 mg/kg in carboxy methyl cellulose) for 10, 20, 40 and 60 days in 24 adult male Sprague Dawley rats. Six rats from control and experimental groups were sacrificed at 10, 20, 40 and 60 days. Confirmation of PD occurrence was done through tyrosine hydroxylase (TH) immune staining of the substantia nigra. Levels of MDA and GSH in the retina were assessed. The retinal sections were processed for histological and immune histochemical staining by anti TH, anti Lc3II, anti SQSTM1/P62 and anti phospho α-Syn. The results showed elevated levels of MDA and decreased levels of GSH in the retina. There is also affection of the dopaminergic neurons in the retina with over expression of Lc3II, phospho α-Syn and decreased expression of SQSTM1/P62.

INTRODUCTION:

Parkinson's disease (PD) is the world's second most prevalent neurodegenerative illness after Alzheimer's disease (AD), defined by the loss of dopaminergic neurons in the substantia nigra, resulting in symptoms of tremor, rigidity, and slowed movement **(Blauwendraat et al., 2020)**.

Alpha-synuclein (α-Syn) is one of the most prevalent neuronal proteins, making up to 0.5–1% of the total protein in the brain and is enriched in presynaptic terminals, giving the normal brain its characteristic punctate neuropil pattern **(Lashuel et al., 2013)**. α-Syn undergoes substantial post-translational modifications (PTMs) that influence its aggregation and toxicity, both of which are important contributors to PD pathogenesis **(Nguyen et al., 2021)**. Phosphorylation of α-Syn is important for oligomer formation, fibrillation, LB formation, and neurotoxicity in Parkinson's disease **(Paleologou et al., 2010)**. The phosphorylation of α-Syn at Ser129 is thought to be important in the production of pathologic inclusions in Parkinson's disease **(Smith et al., 2005)**.

The autophagy–lysosome pathway (ALP) [macroautophagy, microautophagy and chaperone-mediated autophagy], is thought to be involved in the breakdown of α-Syn and its many oligomeric forms. Impairment of autophagy can lead to an accumulation of α-Syn, which can lead to PD and other synucleinopathies **(Stefanis et al., 2019)**. It was reported that Celastrol prevents dopaminergic neuronal death by promoting the development of autophagosomes and eliminating defective mitochondria by autophagy, it implies that one of the key PD therapy targets is stimulation of autophagy **(Lin et al., 2019)**.

The retina is known as the "window to the brain". Any abnormalities in the brain have an impact on the retinal layers and their function **(Devi et al., 2020)**. Many diseases, such as Parkinson's disease (PD), Alzheimer's disease, and glaucoma, are linked to brain and retinal disorders **(Zhou et al., 2017)**. Understanding the disease process and identifying biomarkers in PD might benefit from early diagnosis and disease-modifying medications **(Le et al., 2017)**. The retina is a possible biomarker in neurodegenerative illnesses because imaging techniques are a good diagnostic tool for identifying the intimate link between the eye and the brain **(Lizarán et al., 2018)**.

In order to induce a model of PD, rotenone is a good choice which is a naturally occurring chemical derived from roots, seeds, and stems of various tropical plants, such as the Derris, Tephrosia, Lonchocarpus, and Mundulea species **(Heinz et al., 2017)**. Rotenone can mediate neuronal cell damage through inflammation process, it was proved that rotenone increases production of proinflammatory cytokines such as interleukin (IL) 1 and 6 and tumor necrosis factor (TNF) **(Liang et al., 2017)**. Through structural invasion, the release of pro-inflammatory cytokines, reactive oxygen species (ROS), inducible nitric oxide synthase

(iNOS), and the levels of nitric oxide (NO) and superoxides, which have detrimental effects on dopaminergic neurons, inflammatory activation of microglial cells may contribute to the neurodegenerative process of Parkinson's disease **(Callizot et al., 2019)**.

We sought in this study to assess the possible role of autophagy in the pathogenesis of PD in the retina.

MATERIALS AND METHODS:

Experimental animals:

Forty-eight adult male Sprague Dawley rats weighing 250-300 grams were used in this study. Animals were kept on a standard 12-hr light/dark cycle for 1 week before initiating the experiment. They were housed and allowed free access to water and food (standard rodent chow). This work was carried out at Mansoura experimental research center (MERC), Egypt. The experiment was performed in compliance with the guidelines of the National Institutes of Health (NIH) for the maintenance and use of animals. The present study was approved by the Institutional Research Board (IRB) (code number: MDP.21.09.75), Faculty of Medicine, Mansoura University.

Experimental design:

Rats were randomly divided after one week of acclimatization into control and experimental groups. Control groups (n = 24): The rats were randomly divided into 4 subgroups, each of them included 6 rats. They received daily intraperitoneal (IP) administration of vehicle (1 ml/kg glyceryl trioctanoate, Sigma-Aldrich, Germany) for 10, 20, 40 and 60 days. Experimental groups (n = 24): The rats were randomly divided into 4 subgroups, each of them included 6 rats. They received daily IP rotenone (2.5 mg/kg in carboxy methyl cellulose) **(Normando et al., 2016)** for 10, 20, 40 and 60 days. The rotenone was obtained in powder from Sigma-Aldrich, Germany while the carboxy methyl cellulose was obtained from El-Gomhorya Company for pharmaceuticals, Egypt.

Rats body weight was followed up at start of the study, weekly during it and finally at time of sacrification.

Evaluation of behavioral locomotor activity using the rotarod test (Mouzon et al., 2012):

On the day of testing, rats were kept in their home cages and acclimate to the testing room for at least 15 min (acclimation phase). The rats were placed on the lanes and allowed to walk forward to keep balance. The rod was initially rotating at 4rpm then it was accelerated to 40 rpm in 300 sec. The latency at which each rat had fallen was recorded. The rat was removed and placed back to the home cage. A score was given to each rat as follow; score 1=fall from 1-5 sec, score 2= fall from 6-10 sec, score 3= fall from 11-20 sec, score 4= fall from 21-30 sec, score 5= fall after 30 sec.

Specimen collection

At the assigned time for sacrification of each group, rats were anaesthetized by intraperitoneal injection of 350 mg/kg chloral hydrate 5% **(Maratova et al., 2018)** and were sacrificed by intraperitoneal injection of overdose of sodium thiopental **(Bahrami et al., 2018)**. Eyes were enucleated and the brains were carefully removed.

Each eye was placed in 100 ml of Davidson's fixative solution (2 ml formaldehyde (37%), 35 ml 100% ethanol, 10 ml glacial acetic acid (99.7%) and 53 ml distilled water). The eyes were left for post-fixation at room temperature for 18-36 hr. They were transferred into 50% ethanol solution for 6-8 hr. and then finally to 70% ethanol solution. Samples were refrigerated at 4 °C and stored until dissection **(Tokuda et al., 2018)**.

The eyes were dissected quickly under the stereo microscope. The eyeball was cut posteriorly to the limbus, and thereafter the anterior segment was discarded. The vitreous was removed, and the retina was carefully dissected from the sclera and choroid **(Dilsiz et al., 2006)**, then processed for neurochemical studies (estimation of malondialdehyde MDA and reduced glutathione GSH), histological studies (Hematoxylin and Eosin H&E) and immunohistochemical studies (anti tyrosine hydroxylase (TH), anti-light chain 3 (LC3), anti SQSTM1/P62 and anti-phospho alpha-synculein).

The midbrains were dissected out, cut horizontally, and were processed for paraffin sections and immunohistochemical stained by anti TH.

Biochemical analysis (Sadikan et al., 2022):

Oxidative stress evaluation:

Oxidative stress markers: MDA was measured according to the method of **Ohkawa et al. (1979)** and GSH was measured according to the method of **Tietze (1969)** in retinal tissue homogenate. The kits were purchased from Biodiagnostic, Egypt.

Histological studies:

Paraffin sections of the retina were stained by hematoxylin and eosin to evaluate the main histopathological findings among various experimental groups.

Immunohistochemical studies:

Sections were dewaxed in xylene, rehydrated, and incubated in 3% hydrogen peroxide to inactivate endogenous peroxidase. Sections were treated for 30 min with 10 mM citrate-buffer, (PH 6.0), at 95 ◦C. Sections were incubated with primary antibody rabbit polyclonal anti-tyrosine hydroxylase (Abcam, Egypt at 1:200 dilution), rabbit polyclonal anti-light

chain three II (LC3II) (YPA1652, Chongqing Biospes, China at 1:400-800 dilution), rabbit polyclonal anti-SQSTM1/P62 (YPA1785, Chongqing Biospes, China at 1:400-800 dilution) and rabbit polyclonal anti-phospho α-synculein (YPA2438, Chongqing Biospes, China at 1:25-100 dilution) at 4 ◦C overnight. The next day, slides were washed in phosphate buffered saline and then incubated with secondary antibody. The slides were stained with diaminobenzidine (DAB) (rabbit HRP/DAB (ABC) detection IHC kit, ab64264, Abcam, UK) and the immunoreactivity was visualized as a brown color. Sections were counterstained with hematoxylin.

Image analysis and measurements:

For each animal in all groups, five randomized sections (5 µm thick) were examined. Images were captured with ×40 objective lens using a Leica Q-Win digital camera CH-9435 DFC 290 coupled to a photomicroscope (Germany). We used image J (Version 1.46i, NIH) to perform the measurements and image analysis. In the substantia nigra compacta (SNc), the number of TH-positive dopaminergic neurons was counted per 403,302 μm^2 (high power field area, ×400)**.** In the retina, the linear density of the ganglion cells was estimated by counting the cells per 230 µm length. The thickness of the inner plexiform layer (IPL), inner nuclear layer (INL), outer plexiform layer (OPL), outer nuclear layer (ONL) was measured in µm. The optical density and area percentage of the phospho α-synuclein, LC3II, SQSTM1/P62 and TH immunexpression were measured. In the deconvoluted DAB image, H-DAB-vector was used to yield three differently colored images: green, brown, and blue. Calibration of the DAB images with brown color was performed through measuring of the mean intensity of five non-overlapping areas of the stained tissue **(Varghese et al., 2014)**. The uniformity of section thickness was considered for legitimate comparisons. The empty areas were omitted from the measurements to not bias the outcomes. The intensity numbers were converted into OD through the following formula **(Almasry et al., 2018):**

$$OD = \log \left(\frac{\text{max intensity}}{\text{mean intensity}}\right)$$

where the max intensity = 250; mean intensity = mean gray value

The area percentage of the brown color was measured also in the DAB images. Each image was changed into 8-bit type (gray) then processed into binary (black and white) color image. The measurement icon was calibrated to calculate the area of the field (total epithelial area) and area fraction which was area of the object in the field (black color representing DAB stain) **(Safadi et al., 2010)**.

Statistical analysis:

Data analysis was performed by SPSS software, version 25 (SPSS Inc., PASW statistics for windows version 25. Chicago: SPSS Inc.). Quantitative data were described using mean ± standard deviation for normally distributed data after testing

normality using Shapiro Wilk test. Significance of the obtained results was judged at the (≤0.05) level.

- Student t test was used to compare two independent groups for normally distributed data.
- One Way ANOVA test was used to compare more than 2 independent groups with Post Hoc Tukey test to detect pairwise comparison.

Values were considered as statistically significant if p value ≤ 0.050.

RESULTS:

Assessment of the body weights:

No significant difference was reported in the body weights among the control and experimental groups for the same period **(Histogram. 1, A)**.

Behavioral assessment by the rotarod test:

There was significant difference between the time (in seconds) stayed on the rotating rod among the rotenone-injected groups for 10 days (58.17±10.38), 20 days (34.33±5.43), 40 days (22.0±7.46) and 60 days (6.67±4.23). Also, there was a significant difference among the control and experimental groups for the same period. There was no significant difference between the control groups over the time of the experiment **(Histogram. 1, B)**.

Biochemical results:

The level of the MDA (nmol/g. tissue) in the retina showed progressive significant increase (P<0.05) with prolongation of the period of exposure to rotenone for 10 days (4.15±0.72), 20 days (6.03±0.59), 40 days (8.14±0.52) and 60 days (9.03±0.503). The experimental groups showed significant differences from control at all the time periods **(Histogram. 1, C)**.

The level of GSH (mmol/g. tissue) among the rotenone-injected groups was progressively decreased after injection for 10 days (1.40±0.07), 20 days (1.19±0.09), 40 days (1.06±0.014) and 60 days (0.748±0.17). The experimental groups showed significant reduction in comparison to control at all the time periods **(Histogram. 1, D)**.

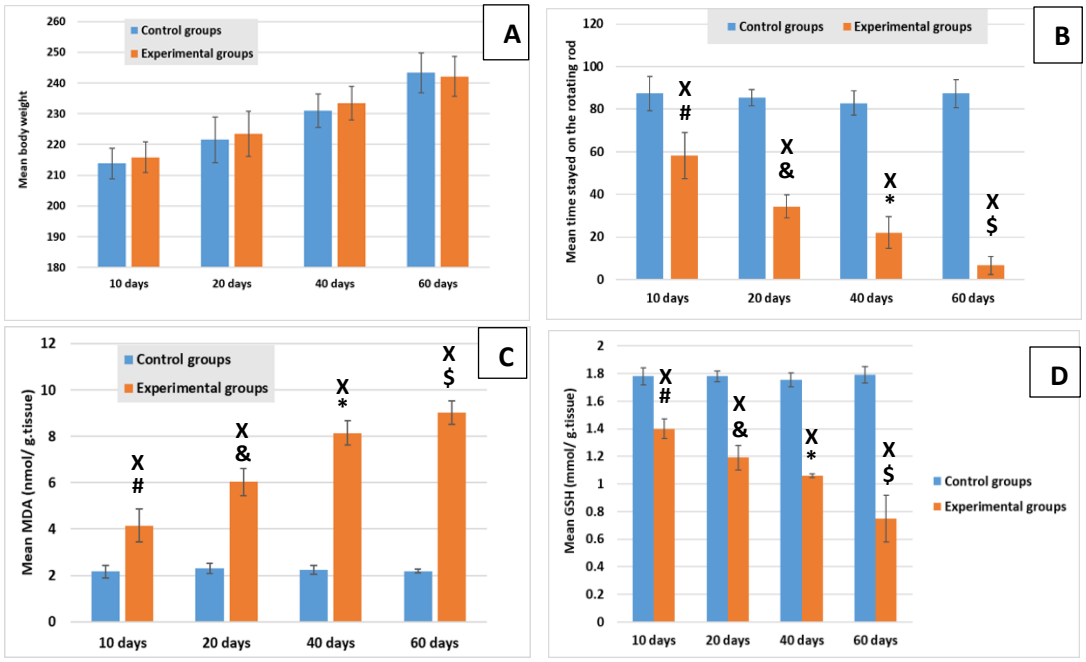

Histogram (1): comparison of mean values, between control and experimental groups and between groups at different sacrification times, of: A) the body weights **(gm)**, B) the time stayed on the rotating rod **(sec),** C) the level of MDA **(nmol/ g. tissue)**, and D) the level of GSH **(mmol/ g. tissue)**. # P<0.001 in comparison to 10 days control group. & p<0.001 in comparison to 20 days control group. * p<0.001 in comparison to 40 days control group. $ p<0.001 in comparison to 60 days control group. X P<0.001 in comparison to other experimental groups.

Histological results:

Rotenone-induced changes in the retinal structure:

Control group showed normal histological structure of well-organized retinal layers **(Fig. 1 A)**. No apparent changes were observed in the rotenone-injected group for 10 and 20 days **(Fig. 1 B, C)**. After 40 days of rotenone injection, ganglion cells became fewer with thickened congested blood vessels within the layer. The INL showed widening in the intranuclear spaces with some blood vessels within it. The OPL became thinner with some degree of focal displacement from the ONL to it. The ONL showed widening in the intranuclear spaces **(Fig. 1 D)**. These changes became more evident in the rotenone-injected group for 60 days **(Fig. 1 E)**.

The linear density of the ganglion cells was significantly decreased with increased exposure to rotenone for 10 days (13.33±1.03), 20 days (11.0±0.89), 40 days (7.83±1.17) and 60 days (5.17±1.47). The linear density in experimental groups was significantly reduced in comparison to control at all the time periods **(Histogram. 2)**.

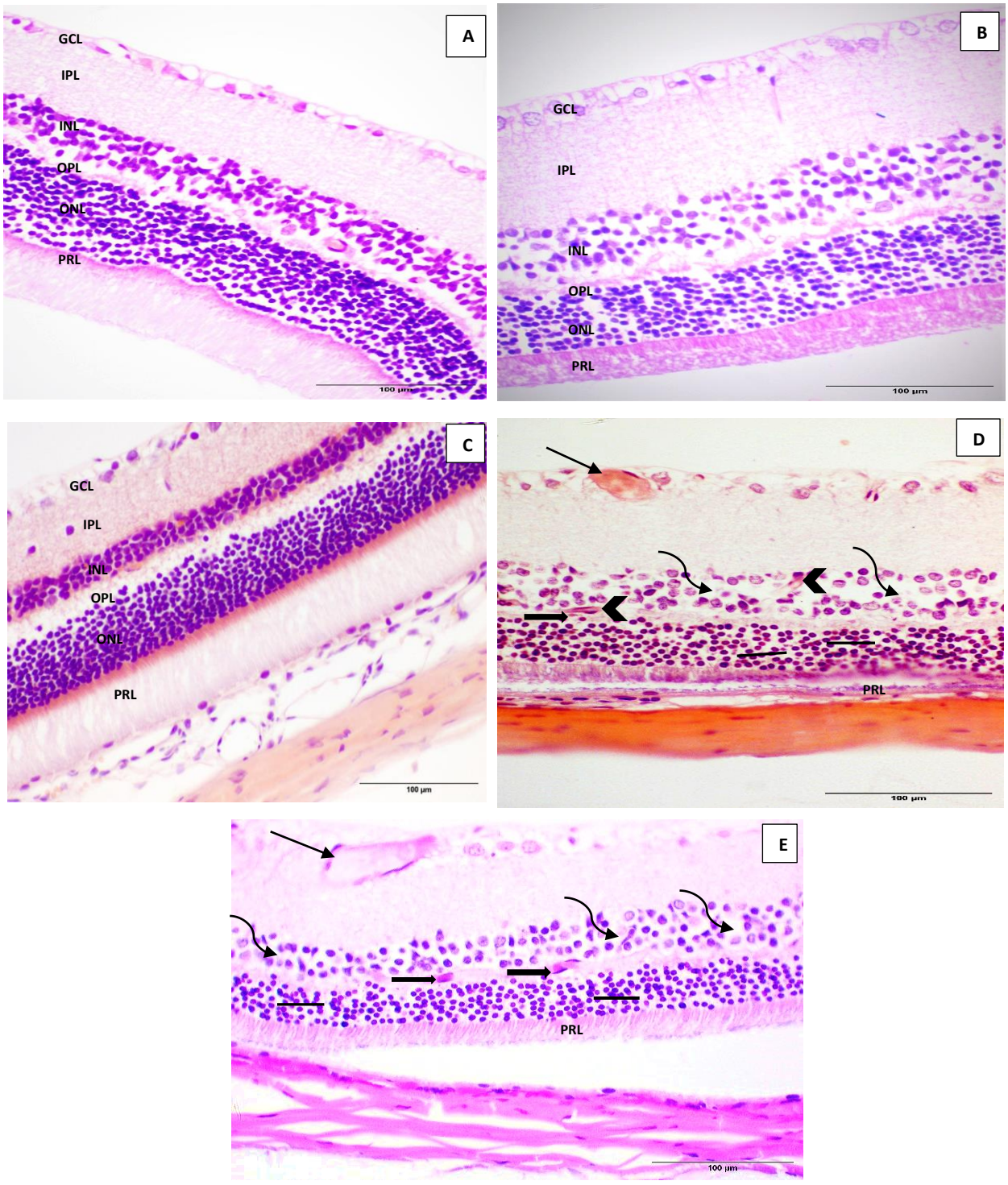

Fig. 1: photomicrographs of Hx&E- stained retinal sections show well-organized retinal layers; in control group **(A)**, rotenone-injected group for 10 days **(B)** and rotenone-injected

group for 20 days **(C)**. Rotenone-injected groups for 40 and 60 days **(D, E)** show a thickened congested blood vessel **(arrow)** in the GCL with decreased number of ganglion cells, widening in intranuclear spaces **(wavy arrows)** and blood vessels within the INL **(arrows heads)**, decreased thickness of the OPL with some focal displacement from the ONL to it **(block arrows)**, widening in the spaces within the ONL **(lines). GCL**, ganglion cell layer, **IPL**, inner plexiform layer, **INL**, inner nuclear layer, **OPL**, outer plexiform layer, **ONL,** outer nuclear layer and **PRL**, photoreceptor layer. (Scale bar = 100 µm) (Magnification, ×400).

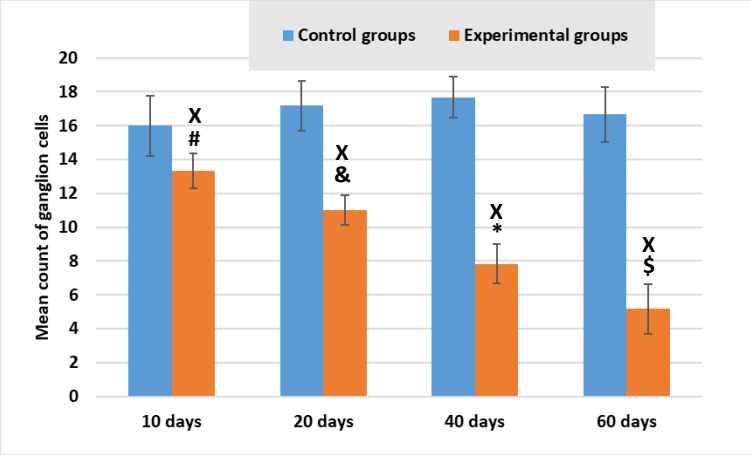

Histogram (2): The linear density of ganglion cells in the experimental groups. # P=0.001 in comparison to 10 days control group. & p<0.001 in comparison to 20 days control group. * p<0.001 in comparison to 40 days control group. $ p<0.001 in comparison to 60 days control group. X P<0.001 in comparison between the experimental groups at different periods.

The thickness of the layers of the retina was significantly reduced in the experimental groups when compared with time-matched control groups. Prolongation of exposure to rotenone was accompanied by a significant decrease in the thickness of the different layers **(Histogram. 3)**.

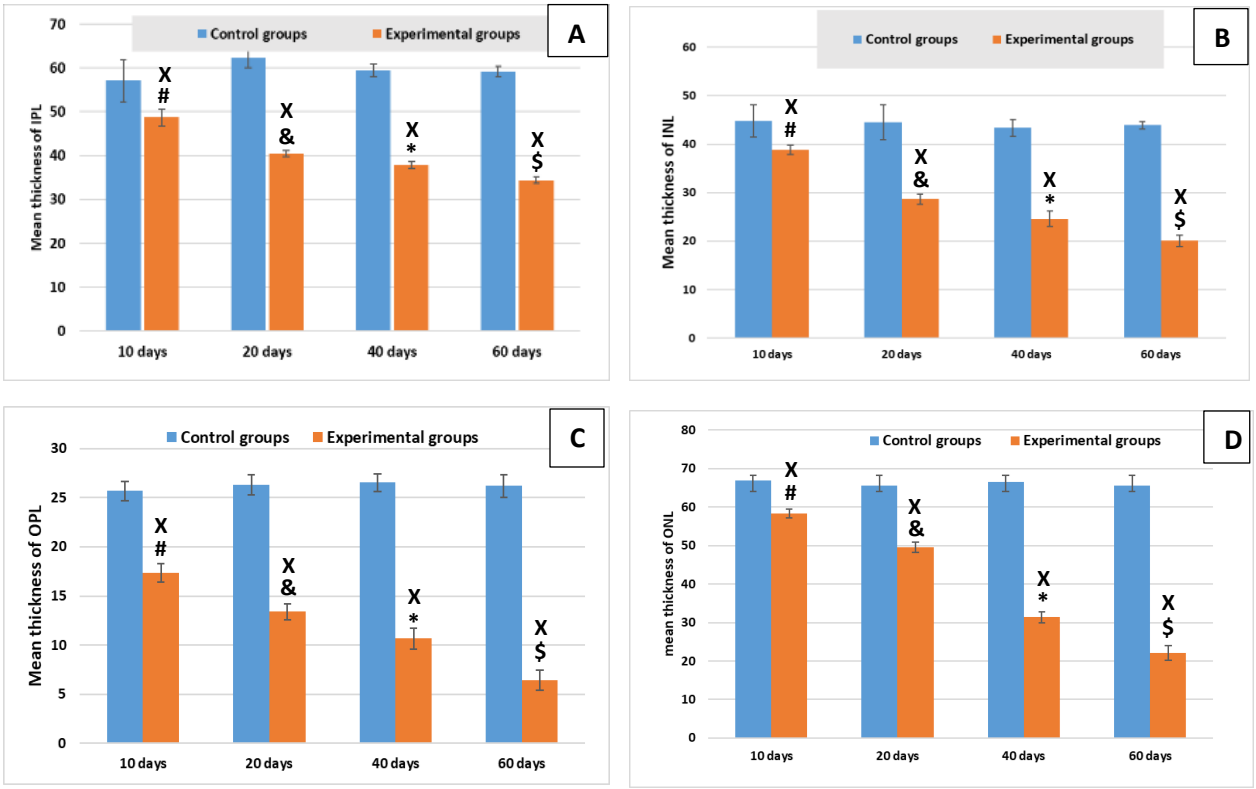

Histogram (3): The mean values of the thickness **(µm)** of A) the IPL, B) the INL, C) the OPL, and D) the ONL in the experimental groups. # p<0.001 in comparison to 10 days control group. & p<0.001 in comparison to 20 days control group. * p<0.001 in comparison to 40 days control group. $ p<0.001 in comparison to 60 days control group. X P<0.001 in comparison between the experimental groups at different periods.

Immunohistochemical results:

Evaluation of tyrosine hydroxylase immune expression in the substantia nigra:

TH immunoreactivity in the SNc of control **(Fig. 2 A)** and rotenone-injected groups for 10 days **(Fig. 2 B)** was observed as strong positive reaction of the dopaminergic neurons. Group injected with rotenone for 20 days showed moderate positive immune reaction of the dopaminergic neurons **(Fig. 2 C)**. The reaction was weak in the Rotenone-injected groups for 40 **(Fig. 2 D)** and 60 days **(Fig. 2 E)**.

Morphometric study of the mean count of the dopaminergic neurons in the SNc:

The mean count of the dopaminergic neurons in the SNc was significantly reduced in the experimental groups when compared with time-matched control groups. Prolongation

of exposure to rotenone was accompanied by a significant decrease in the number of dopaminergic neurons in SNc **(Fig. 2F)**.

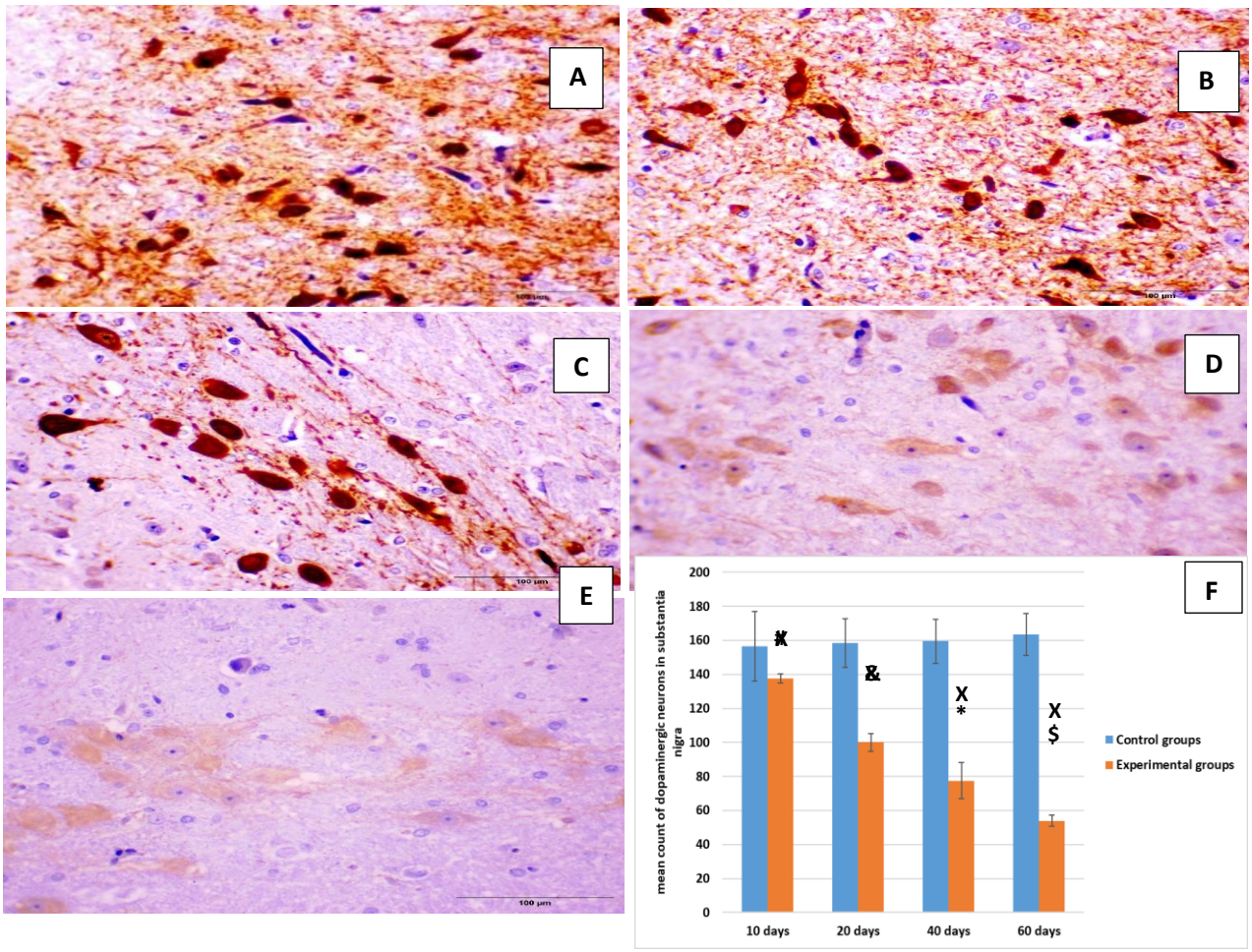

Fig. 2: photomicrographs of the TH-stained sections of the substantia nigra show strong positive immune reaction of the dopaminergic neurons in the control **(A)** and rotenone-injected groups for 10 days **(B)**. There is a moderate positive immune reaction of the dopaminergic neurons in the rotenone-injected group for 20 days **(C)**. Both rotenone-injected groups for 40 days **(D)** and 60 days **(E)** show a weak positive immune reaction of the dopaminergic neurons. (Scale bar = 100 µm) (Magnification, ×400) **(F)**: Histogram showing the mean values of count of the dopaminergic neurons in the experimental groups. # p=0.048 in comparison to 10 days control group. & p<0.001 in comparison to 20 days control group. * p<0.001 in comparison to 40 days control group. $ p<0.001 in comparison to 60 days control group. X P<0.001 in comparison between the experimental groups at different periods

Evaluation of tyrosine hydroxylase immune expression in the retina:

There was a strong positive immunoreactivity in the control **(Fig. 3 A)** and rotenone injected groups for 10 **(Fig. 3 B)** and 20 days **(Fig. 3 C)** within all the layers of the retina.

A moderate positive immune expression is shown within the GCL, IPL and PRL in the group injected by rotenone for 40 days **(Fig. 3 D)** and within the GCL in the rotenone-injected group for 60 days **(Fig. 3 E)**.

Morphometric study of the mean values of area percentage and optical density of TH in the retina:

The mean values of the area percentage and optical density of the TH were significantly decreased in the experimental groups compared to the controls of the same period. Prolongation of the duration of rotenone injection made the decrease more significant **(Fig. 3 F, G)**.

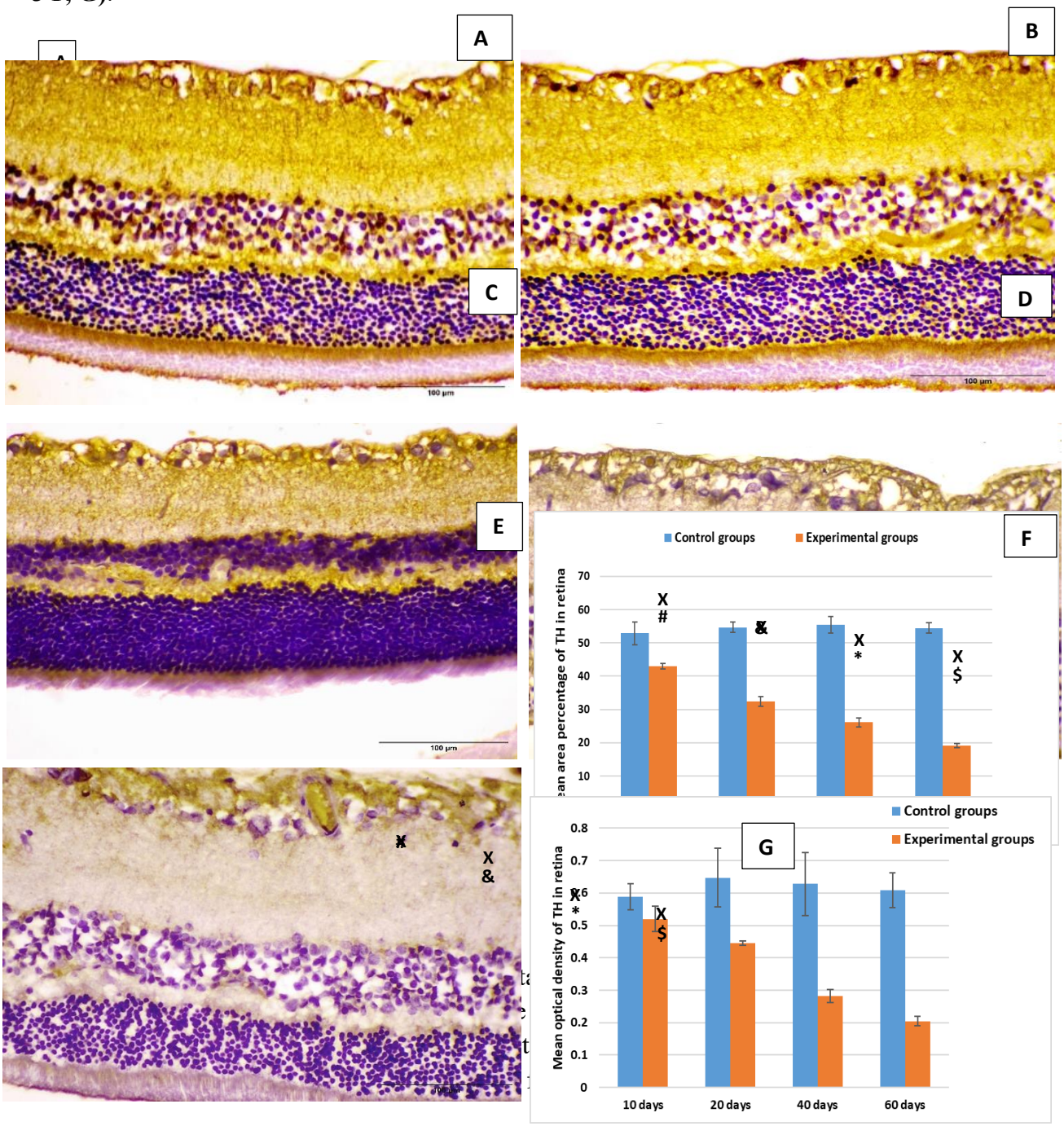

rotenone-injected group for 60 days **(E)**. (Scale bar = 100 µm) (Magnification, ×400) **(F)**: Histogram showing the mean values of area percentage of TH in the experimental groups $^{\#}$ $p<0.001$ in comparison to 10 days control group. $^{\&}$ $p<0.001$ in comparison to 20 days control group. * $p<0.001$ in comparison to 40 days control group. $^{\$}$ $p<0.001$ in comparison to 60 days control group. ^{X} $p<0.001$ in comparison between the experimental groups at different periods. **(G)**: Histogram showing the mean values of optical density of TH in the experimental groups $^{\#}$ $p=0.02$ in comparison to 10 days control group. $^{\&}$ $p<0.001$ in comparison to 20 days control group. * $p<0.001$ in comparison to 40 days control group. $^{\$}$ $p<0.001$ in comparison to 60 days control group. ^{X} $P<0.001$ in comparison between the experimental groups at different periods.

Evaluation of Lc3II immune expression in the retina:

Control group showed negative immune expression within the layers **(Fig. 4 A)**. There was a weak positive immune reaction within the GCL in rotenone-injected group for 10 days **(Fig. 4 B)** and within the GCL, IPL and OPL in group injected for 20 days **(Fig. 4 C)**. Rotenone-injected group for 40 days showed moderate positive immune expression within the GCL, IPL and OPL **(Fig. 4 D)** while group injected for 60 days had strong positive immune expression within the GCL, IPL, OPL and ONL **(Fig. 4 E)**.

Morphometric study of the mean values of area percentage and optical density of Lc3II in the retina:

There was a significant increase in the area percentage and optical density of LC3 II among the experimental groups compared to the controls of the same period. The more the duration of exposure to rotenone, the more the significant increase **(Fig. 4 F, G)**.

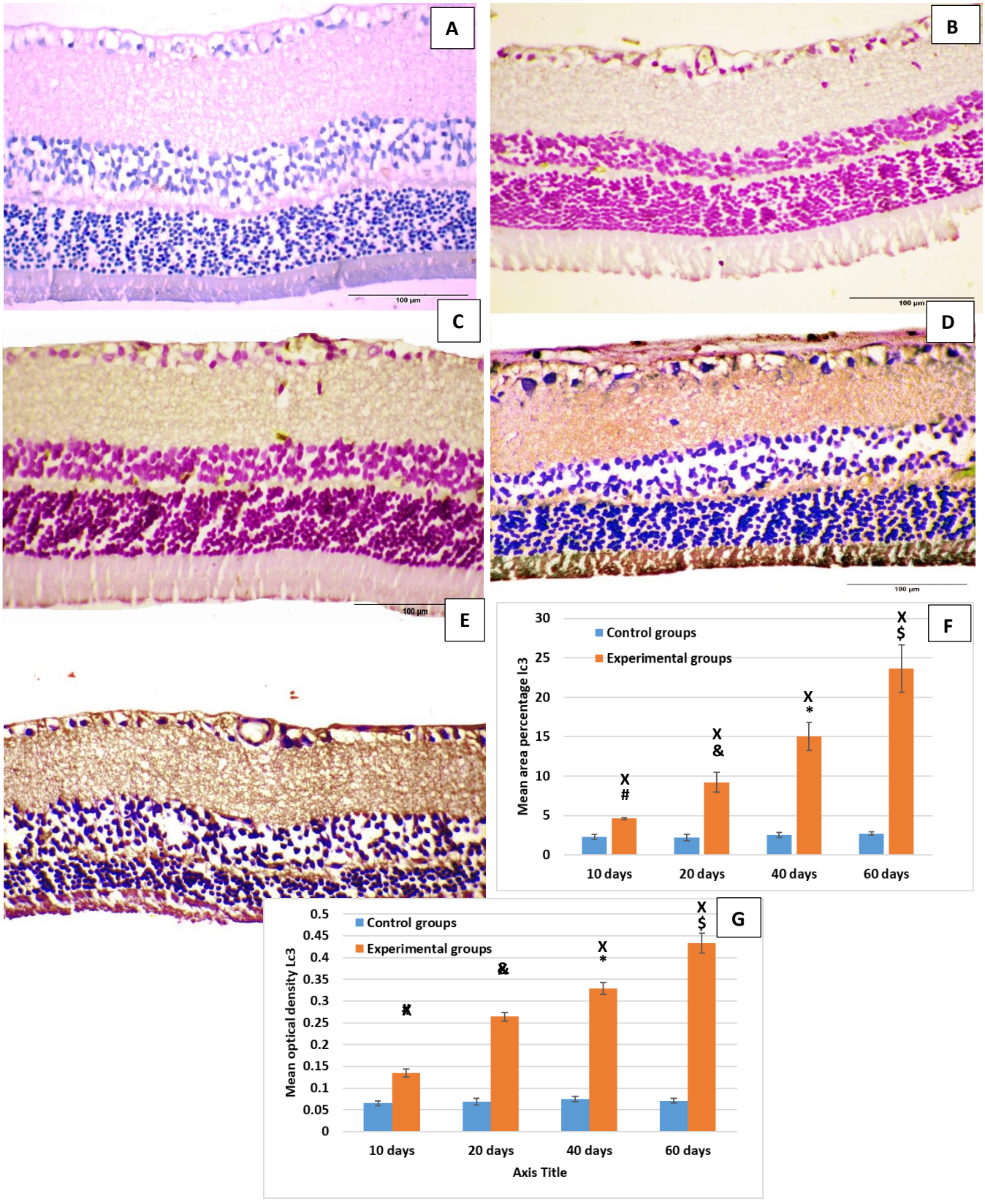
A
B
C
D
E
F
G
100 µm
Control groups
Experimental groups
Mean area percentage lc3
10 days
20 days
40 days
60 days
Mean optical density Lc3
Axis Title

Fig. 4: photomicrographs of the LC3II immune stained retinal sections show negative immune expression within the layers of the control retina **(A)**. There is a weak positive immune expression within the GCL in the rotenone-injected group for 10 days **(B)** and within the GCL, IPL and OPL in rotenone-injected group for 20 days **(C)**. There is moderate positive immune expression within the GCL, IPL and OPL and strong positive immune expression within the PRL in the rotenone-injected group for 40 days **(D)**. Rotenone-injected group for 60 days shows strong positive immune expression within the GCL, IPL, OPL and PRL **(E)**. (Scale bar = 100 μm) (Magnification, ×400). **(F)**: Histogram showing the mean values of area percentage of Lc3II in the experimental groups. **(G)**: Histogram showing the mean values of optical density of Lc3II in the experimental groups. $^{\#}$ $p<0.001$ in comparison to 10 days control group. $^{\&}$ $p<0.001$ in comparison to 20 days control group. * $p<0.001$ in comparison to 40 days control group. $^{\$}$ $p<0.001$ in comparison to 60 days control group. ^{X} $p<0.001$ in comparison between the experimental groups at different periods.

Evaluation of SQSTM1/P62 immune expression in the retina:

SQSTM1/P62 immune stained retinal sections of control **(Fig. 5 A)** and rotenone-injected groups for 10 **(Fig. 5 B)** and 20 days **(Fig. 5 C)** showed strong positive immune expression within the GCL, IPL, OPL and PRL, group injected for 40 days had moderate positive immune expression within the GCL and IPL **(Fig. 5 D)**. Rotenone-injected group for 60 days showed weak positive immune expression within the GCL, IPL, OPL and PRL **(Fig. 5 E)**.

Morphometric study of the mean values of area percentage and optical density of SQSTM1/P62 in the retina:

The area percentage and optical density of SQSTM1/P62 in the retina showed significant reduction in the experimental compared to the control groups with decreasing the levels of expression with prolongation of the duration of exposure to rotenone **(Fig. 5 F, G)**.

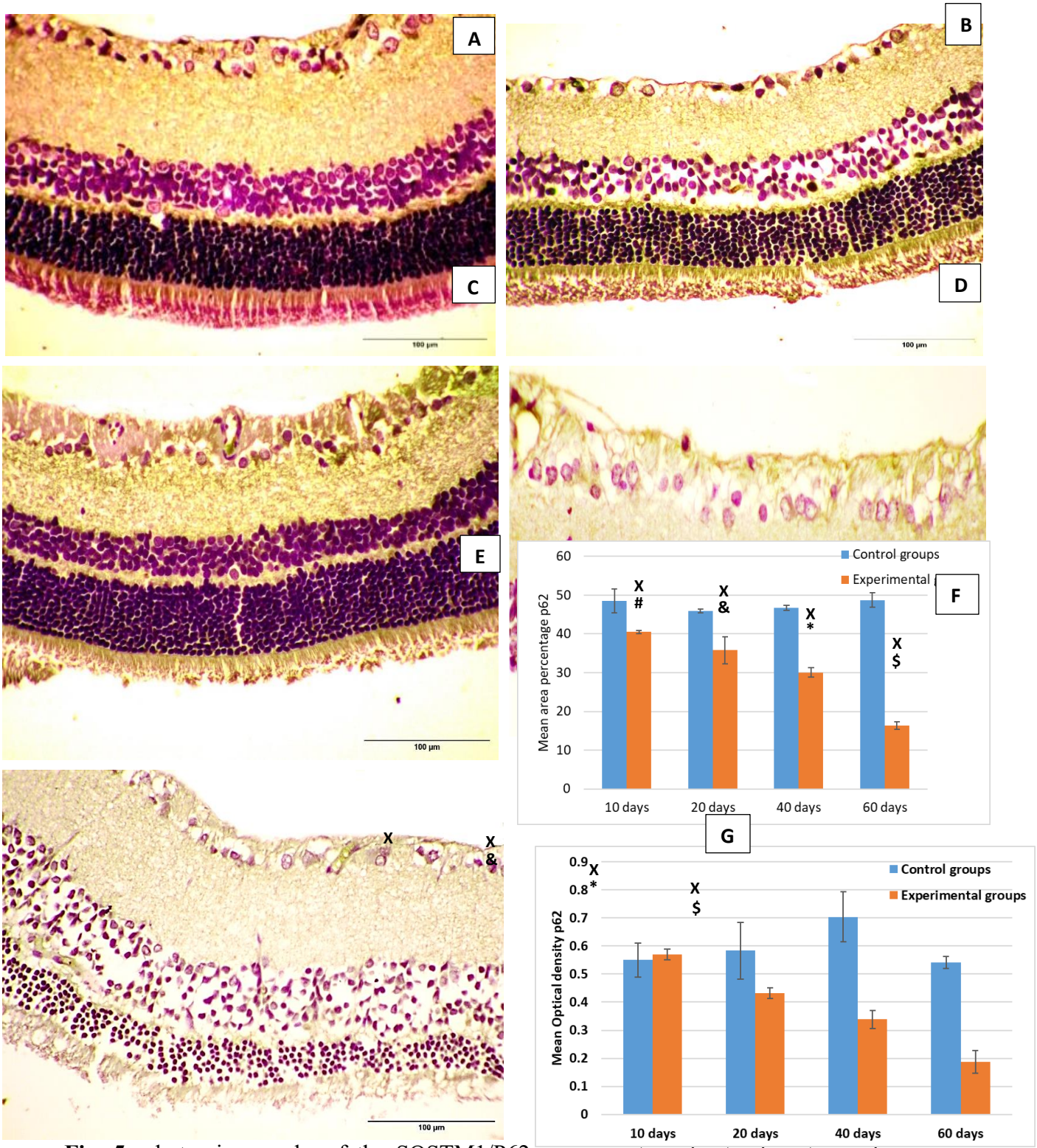

Fig. 5: photomicrographs of the SQSTM1/P62 immune stained retinal sections show strong positive immune expression within the GCL, IPL, OPL and PRL in the control **(A)** and rotenone-injected groups for 10 **(B)** and 20 **(C)** days. There is a moderate positive

immune expression within the GCL and IPL in the rotenone-injected group for 40 days **(D)**. Rotenone-injected group for 60 days shows a weak positive immune expression within the GCL, IPL, OPL and PRL **(E)** (Scale bar = 100 μm) (Magnification, ×400). **(F)**: Histogram showing the mean values of area percentage of SQSTM1/P62 in the experimental groups. # $p<0.001$ in comparison to 10 days control group. & $p<0.001$ in comparison to 20 days control group. * $p<0.001$ in comparison to 40 days control group. $ $p<0.001$ in comparison to 60 days control group. X $p<0.001$ in comparison between the experimental groups at different periods. **(G)**: Histogram showing the mean values of optical density of SQSTM1/P62 in the experimental groups. & $p=0.005$ in comparison to 20 days control group. * $p<0.001$ in comparison to 40 days control group. $ $p<0.001$ in comparison to 60 days control group. X $p<0.001$ in comparison between the experimental groups at different periods.

Evaluation of Phospho α-synculein immune expression in the retina:

Phospho α-synculein immune stained retinal sections of control group showed negative immune expression within the layers **(Fig. 6 A)**, rotenone-injected rats for 10 days had weak positive immune expression within the PRL **(Fig. 6 B)**. Group injected by rotenone for 20 days showed moderate positive immune expression within the GCL, IPL, OPL and PRL **(Fig. 6 C)**. Rotenone-injected rats for 40 days showed moderate positive immune expression within the GCL, IPL and OPL with strong positive immune expression within the PRL **(Fig. 6 D)**. Rats injected with rotenone for 60 days showed strong positive immune expression within the GCL, IPL, OPL and PRL **(Fig. 6 E)**.

Morphometric study of the mean values of area percentage and optical density of Phospho α-synculein in the retina:

There is a significant elevation of area percentage and optical density immune expression of phosphorylated α-synuclein at Ser129 in the retina of the rotenone-injected rats compared to the controls. There was a positive correlation between the duration of the experiment and the level of expression **(Fig. 6 F, G)**.

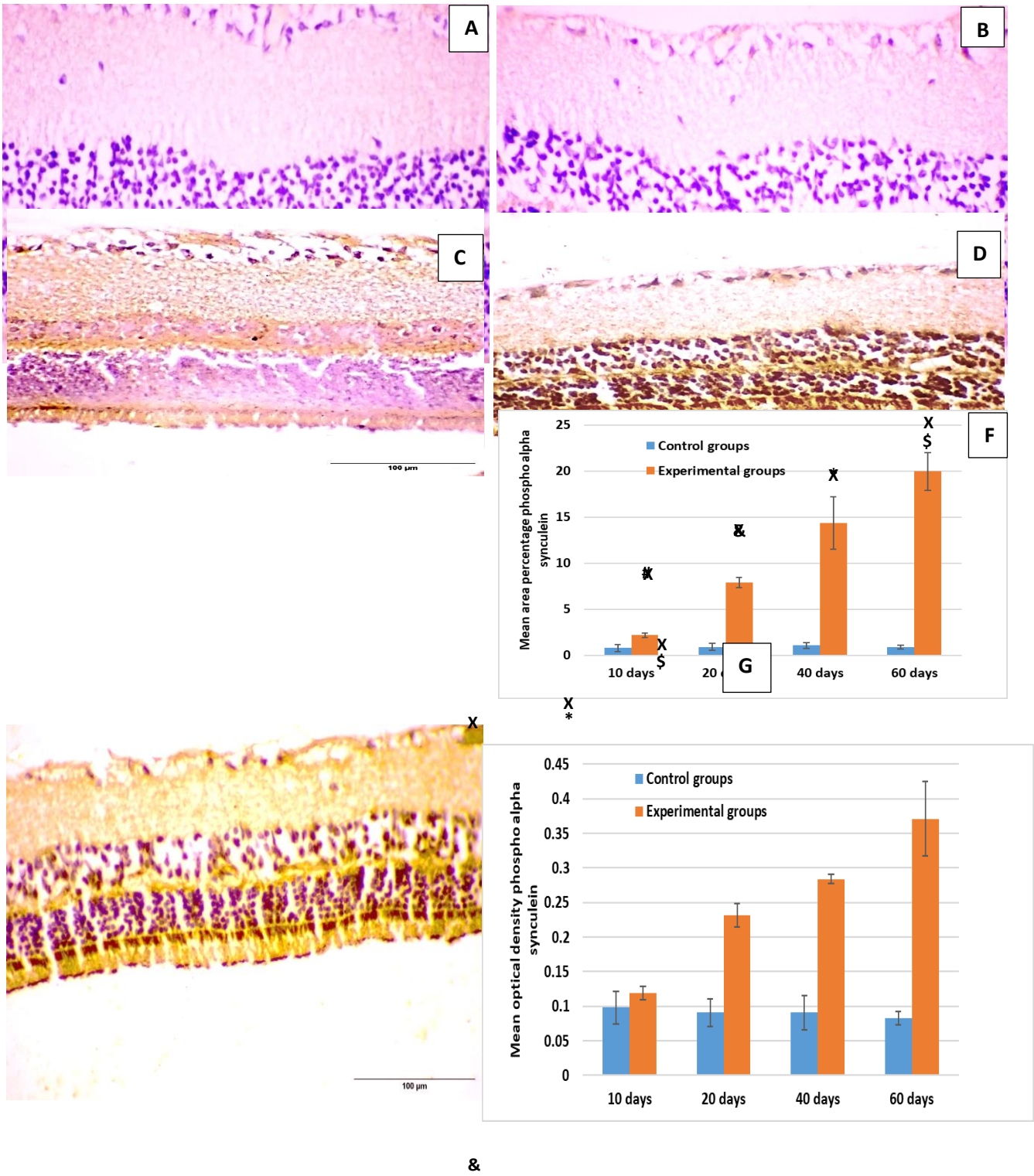

Fig. 6: photomicrographs of the phospho α-synculein immune stained retinal sections show negative immune expression within the layers in the control group **(A)**. There is a weak positive immune expression within the PRL in the rotenone-injected group for 10 days **(B)**.

Rotenone-injected group for 20 days shows a moderate positive immune expression within the GCL, IPL, OPL and PRL **(C)**. There is a strong positive immune expression within the INL, OPL, ONL and PRL in the rotenone-injected group for 40 days **(D)**. Strong positive immune expression within the GCL, IPL, OPL and PRL is found in the rotenone-injected group for 60 days **(E)**. (Scale bar = 100 μm) (Magnification, ×400). **(F)**: Histogram showing the mean values of area percentage of phospho α-synculein in the experimental groups. $^{\#}$ $p<0.001$ in comparison to 10 days control group. $^{\&}$ $p<0.001$ in comparison to 20 days control group. * $p<0.001$ in comparison to 40 days control group. $^{\$}$ $p<0.001$ in comparison to 60 days control group. ^{X} $p<0.001$ in comparison between the experimental groups at different periods. **(G)**: Histogram showing the mean values of optical density of phospho α-synculein in the experimental groups. $^{\&}$ $p<0.001$ in comparison to 20 days control group. * $p<0.001$ in comparison to 40 days control group. $^{\$}$ $p<0.001$ in comparison to 60 days control group. ^{X} $p<0.001$ in comparison between the experimental groups at different periods.

Discussion:

This study aimed to demonstrate the possible role of the autophagy in the pathogenesis of the Parkinson's diseases through evaluating their histopathological effects on the retina.

We induced the rotenone-model of Parkinson disease successfully, that has been proven by the significant reduction in the tyrosine hydroxylase (TH) stained neurons in the substantia nigra of experimental compared to the control groups and with increasing the duration of exposure. The locomotor activity was also significantly reduced in the experimental groups compared to the controls. Likewise, the time the rats stayed on the rotating rod was significantly reduced with increasing the duration of exposure to rotenone. These changes result from the selective loss of the dopaminergic neurons that causes rigidity, bradykinesia, postural instability and resting tremors **(Poewe et al., 2017)**.

Parkinson- model did not alter the body weight in relation to control rats for the same period similar to the results of **Abdo et al. (1988)**. However, Santos et al., reported that rotenone administration reduced the body weights of rats compared to the controls **(Santos et al., 2023)**, linking these changes to decreased intestinal transit and motility which are in accordance with the variations in the enteric nervous system **(Bu et al., 2019)**.

Rotenone injection resulted in oxidative stress in the retina as revealed by the significant increase in the levels of MDA and significant decrease in the levels of GSH compared to the controls. Oxidative stress increased also significantly with increasing the period of exposure to rotenone. This is in agreement with previous studies, who attributed oxidative damage associated with PD to DNA damage that causes elevation of the levels of MDA and lower activity of scavenging antioxidant enzymes such as GSH **(Khan & Ali, 2018)**. This oxidative stress yields from two mechanisms, the tyrosine hydroxylase enzyme that

makes the dopaminergic neurons more prone to oxidative stress and the presence of iron in the dopaminergic neurons that increases the production of superoxide radicals and hydrogen peroxide causing oxidative damage **(Umeno et al., 2017)**.

Histological examination of the retina showed a significant decrease in the linear density of the ganglion cells in the experimental compared to the control groups. The reduction was also significantly reduced with the prolongation of rotenone exposure, in accordance with **Altintaş et al. (2008)**. **Tatton et al. (1990)** attributed the primary impairment of vision in PD to the loss of retinal dopaminergic neurons that causes loss of retinal amacrine cells which provide input to retinal ganglion cells.

Rotenone exposure significantly reduced the thickness of the IPL, INL, OPL and ONL in the experimental compared to the control groups. In agreement with the pervious study of Rascunà et al., who proved the occurrence of these retinal changes at early stages of the disease independently from age, sex, history of abnormal blood pressure and using of dopaminergic drugs **(Rascunà et al., 2020)**. **Kirbas et al. (2013)** explained this thinning of the layers of the retina by the role of the dopamine in the retina as a major neurotransmitter and modulator, its level depletes with PD causing these structural changes. On the other hand, **Miri et al. (2016)** observed no difference in this aspect.

Tyrosine hydroxylase (TH) is an ideal marker for the dopaminergic neurons that are ultimately affected with PD in different cell cultures **(Rausch et al., 2022)**. Amacrine cells within the retina are the TH-immunoreactive cells with their cell bodies lie in the INL and GCL and their dendrites ramify in the IPL **(Crooks & Kolb, 1992)**. TH-immunehistochemical staining results showed a significant reduction of immune expression in the experimental compared to the control groups in the retina. **Lizarán et al. (2020)** also demonstrated the loss of the retinal dopaminergic cells and their plexus as a part of the impairment of the global dopaminergic system accompanied with the Parkinson's diseases.

LC3II is a specific marker for autophagosomes formation **(Miki et al., 2018)**. SQSTM1/P62 degradation is widely used as a biochemical marker for autophagy, it acts as a cargo receptor for ubiquitinated protein aggregates that are intended for selective autophagy **(Lamark et al., 2017)**. Immunohistochemical analysis of the retina, in this study, showed significant elevation of the level of immunoexpression of LC3II in the retina of the experimental groups compared to the control. The level of immunoexpression progressively increased with prolongation of the duration of the experiment. The immunoexpression of SQSTM1/P62 in the retina showed significant reduction in the experimental compared to the control groups with decreasing the levels of expression with prolongation of the duration of exposure to rotenone. These finding indicate increase of autophagy in the retina in accordance with Xiong et al. who suggested that autophagy may offer neuroprotection against the rotenone **(Xiong et al., 2013)**. Oxidative stress is considered upstream process of autophagy which is helpful to prevent cellular damage

(Polo et al., 2007). The autophagy can be under the ability to preserve cellular balance with exceeding the pathogenic stress **(Lee & Weihl, 2017)**.

Our study has revealed the significant elevation of immunoexpression of phosphorylated α-synuclein at Ser129 in the retina of the rotenone-injected rats compared to the controls. There was a positive correlation between the duration of the experiment and the level of expression. **Lizarán et al.,** using phosphorylated α-synuclein at Ser129 antibody, demonstrated for the first time the immunoreactivity of phospho α-synuclein in the human retina of PD similar to the brain lewy bodies (LBs) **(Lizarán et al., 2018)**. In the brain, phosphorylation level of α-Syn at Ser129 may be a key event involved in LBs formation and potentially dopaminergic neurodegeneration **(Anderson et al., 2006)**. However, Silveira et al. suggested that phosphorylation does not play an active role in the accumulation of cytotoxic pre-inclusion aggregates, and at the same time, constitutive expression of phosphorylation-mimicking forms of alpha-synuclein does not protect from neurodegeneration **(Silveira et al., 2009)**. The actual effect of phosphorylation of α-Syn is still contested, as different studies show it to either induce neurotoxicity or protect neurons **(Sugeno et al., 2008)**.

Impairment of the ubiquitin–proteasome system or the autophagy–lysosome pathway can induce an accumulation of α-Syn, which can lead to PD and other synucleinopathies. It was recently shown that pS129 α-Syn can operate as a signal for its breakdown, however the mechanism (proteasome or macroautophagy) is unknown **(Arawaka et al., 2017)**. In a yeast model of Parkinson's disease, the S129A mutation hampered α-Syn clearance via the autophagic degradation pathway **(Tenreiro et al., 2014)**. Overexpression of Polo-like kinase 2, the major kinase responsible for α-Syn phosphorylation in the brain, increases α-Syn turnover through the autophagic degradation pathway **(Dahmene et al., 2017)**.

Conclusion:

In this study, we observed a positive correlation between autophagy in the retina and the accumulation of phosphor α-synuclein. Upregulation of autophagy in the retina may act as a protective mechanism to hamper the over expression of the potential biomarker of PD phospho α-synuclein.

References:

Abdo, K. M., Eustis, S. L., Haseman, J., Huff, J. E., Peters, A., & Persing, R. (1988). Toxicity and carcinogenicity of rotenone given in the feed to F344/N rats and B6C3F1 mice for up to two years. *Drug and Chemical Toxicology*, *11*(3), 225–235.

Almasry, S. M., Habib, E. K., Elmansy, R. A., & Hassan, Z. A. (2018). Hyperglycemia alters the protein levels of prominin-1 and VEGFA in the retina of albino rats. *Journal of Histochemistry & Cytochemistry*, *66*(1), 33–45.

Altintaş, Ö., Işeri, P., Özkan, B., & Çağlar, Y. (2008). Correlation between retinal morphological and functional findings and clinical severity in Parkinson's disease. *Documenta Ophthalmologica*, *116*, 137–146.

Anderson, J. P., Walker, D. E., Goldstein, J. M., De Laat, R., Banducci, K., Caccavello, R. J., Barbour, R., Huang, J., Kling, K., & Lee, M. (2006). Phosphorylation of Ser-129 is the dominant pathological modification of α-synuclein in familial and sporadic Lewy body disease. *Journal of Biological Chemistry*, *281*(40), 29739–29752.

Arawaka, S., Sato, H., Sasaki, A., Koyama, S., & Kato, T. (2017). Mechanisms underlying extensive Ser129-phosphorylation in α-synuclein aggregates. *Acta Neuropathologica Communications*, *5*(1), 1–15.

Azeredo da Silveira, S., Schneider, B. L., Cifuentes-Diaz, C., Sage, D., Abbas-Terki, T., Iwatsubo, T., Unser, M., & Aebischer, P. (2009). Phosphorylation does not prompt, nor prevent, the formation of α-synuclein toxic species in a rat model of Parkinson's disease. *Human Molecular Genetics*, *18*(5), 872–887.

Bahrami, R., Akbari, E., Rasras, S., Jazayeri, N., Khodayar, M., Foruozandeh, H., Zeinali, M., Kartalaei, M., Ardeshiri, M., & Baiatinia, F. (2018). Effect of local N-acetyl-cysteine in the prevention of epidural fibrosis in rat laminectomy model. *Asian Journal of Neurosurgery*, *13*(03), 664–668.

Blauwendraat, C., Nalls, M. A., & Singleton, A. B. (2020). The genetic architecture of Parkinson's disease. *The Lancet Neurology*, *19*(2), 170–178. https://doi.org/10.1016/S1474-4422(19)30287-X

Bu, J., Qiao, X., He, Y., & Liu, J. (2019). Colonic electrical stimulation improves colonic transit in rotenone-induced Parkinson's disease model through affecting enteric neurons. *Life Sciences*, *231*, 116581.

Callizot, N., Combes, M., Henriques, A., & Poindron, P. (2019). Necrosis, apoptosis, necroptosis, three modes of action of dopaminergic neuron neurotoxins. *PLoS One*, *14*(4), e0215277.

Crooks, J., & Kolb, H. (1992). Localization of GABA, glycine, glutamate and tyrosine hydroxylase in the human retina. *Journal of Comparative Neurology*, *315*(3), 287–302.

Dahmene, M., Bérard, M., & Oueslati, A. (2017). Dissecting the molecular pathway involved in PLK2 kinase-mediated α-synuclein-selective autophagic degradation. *Journal of Biological Chemistry*, *292*(9), 3919–3928.

Dilsiz, N., Sahaboglu, A., Yıldız, M. Z., & Reichenbach, A. (2006). Protective effects of various antioxidants during ischemia-reperfusion in the rat retina. *Graefe's Archive*

for Clinical and Experimental Ophthalmology, *244*(5), 627–633.

Dos Santos, J. C. C., Rebouças, C. da S. M., Oliveira, L. F., dos Santos Cardoso, F., de Souza Nascimento, T., Oliveira, A. V., Lima, M. P. P., de Andrade, G. M., de Castro Brito, G. A., & de Barros Viana, G. S. (2023). The role of gut-brain axis in a rotenone-induced rat model of Parkinson's disease. *Neurobiology of Aging*, *132*, 185–197.

González-Polo, R. A., Niso-Santano, M., Ortíz-Ortíz, M. A., Gómez-Martín, A., Morán, J. M., García-Rubio, L., Francisco-Morcillo, J., Zaragoza, C., Soler, G., & Fuentes, J. M. (2007). Inhibition of paraquat-induced autophagy accelerates the apoptotic cell death in neuroblastoma SH-SY5Y cells. *Toxicological Sciences*, *97*(2), 448–458.

Heinz, S., Freyberger, A., Lawrenz, B., Schladt, L., Schmuck, G., & Ellinger-Ziegelbauer, H. (2017). Mechanistic investigations of the mitochondrial complex I inhibitor rotenone in the context of pharmacological and safety evaluation. *Scientific Reports*, *7*(1), 1–13.

Khan, Z., & Ali, S. A. (2018). Oxidative stress-related biomarkers in Parkinson's disease: A systematic review and meta-analysis. *Iranian Journal of Neurology*, *17*(3), 137.

Kirbas, S., Turkyilmaz, K., Tufekci, A., & Durmus, M. (2013). Retinal nerve fiber layer thickness in Parkinson disease. *Journal of Neuro-Ophthalmology*, *33*(1), 62–65.

Lamark, T., Svenning, S., & Johansen, T. (2017). Regulation of selective autophagy: the p62/SQSTM1 paradigm. *Essays in Biochemistry*, *61*(6), 609–624.

Lashuel, H. A., Overk, C. R., Oueslati, A., & Masliah, E. (2013). The many faces of α-synuclein: from structure and toxicity to therapeutic target. *Nature Reviews Neuroscience*, *14*(1), 38–48.

Le, W., Dong, J., Li, S., & Korczyn, A. D. (2017). Can biomarkers help the early diagnosis of Parkinson's disease? *Neuroscience Bulletin*, *33*(5), 535–542.

Lee, Y., & Weihl, C. C. (2017). Regulation of SQSTM1/p62 via UBA domain ubiquitination and its role in disease. *Autophagy*, *13*(9), 1615–1616.

Liang, Y., Zhou, T., Chen, Y., Lin, D., Jing, X., Peng, S., Zheng, D., Zeng, Z., Lei, M., & Wu, X. (2017). Rifampicin inhibits rotenone-induced microglial inflammation via enhancement of autophagy. *Neurotoxicology*, *63*, 137–145.

Lin, M.-W., Lin, C. C., Chen, Y.-H., Yang, H.-B., & Hung, S.-Y. (2019). Celastrol inhibits dopaminergic neuronal death of Parkinson's disease through activating mitophagy. *Antioxidants*, *9*(1), 37.

Maratova, K., Soucek, O., Matyskova, J., Hlavka, Z., Petruzelkova, L., Obermannova, B., Pruhova, S., Kolouskova, S., & Sumnik, Z. (2018). Muscle functions and bone

strength are impaired in adolescents with type 1 diabetes. *Bone*, *106*, 22–27.

Miki, Y., Shimoyama, S., Kon, T., Ueno, T., Hayakari, R., Tanji, K., Matsumiya, T., Tsushima, E., Mori, F., & Wakabayashi, K. (2018). Alteration of autophagy-related proteins in peripheral blood mononuclear cells of patients with Parkinson's disease. *Neurobiology of Aging*, *63*, 33–43.

Miri, S., Glazman, S., & Bodis-Wollner, I. (2016). OCT and Parkinson's Disease. *OCT in Central Nervous System Diseases: The Eye as a Window to the Brain*, 105–121.

Mohana Devi, S., Mahalaxmi, I., Aswathy, N. P., Dhivya, V., & Balachandar, V. (2020). Does retina play a role in Parkinson's Disease? *Acta Neurologica Belgica*, *120*(2), 257–265.

Mouzon, B., Chaytow, H., Crynen, G., Bachmeier, C., Stewart, J., Mullan, M., Stewart, W., & Crawford, F. (2012). Repetitive mild traumatic brain injury in a mouse model produces learning and memory deficits accompanied by histological changes. *Journal of Neurotrauma*, *29*(18), 2761–2773.

Nguyen, P. H., Ramamoorthy, A., Sahoo, B. R., Zheng, J., Faller, P., Straub, J. E., Dominguez, L., Shea, J.-E., Dokholyan, N. V, & De Simone, A. (2021). Amyloid oligomers: A joint experimental/computational perspective on Alzheimer's disease, Parkinson's disease, Type II diabetes, and amyotrophic lateral sclerosis. *Chemical Reviews*, *121*(4), 2545–2647.

Normando, E. M., Davis, B. M., De Groef, L., Nizari, S., Turner, L. A., Ravindran, N., Pahlitzsch, M., Brenton, J., Malaguarnera, G., & Guo, L. (2016). The retina as an early biomarker of neurodegeneration in a rotenone-induced model of Parkinson's disease: evidence for a neuroprotective effect of rosiglitazone in the eye and brain. *Acta Neuropathologica Communications*, *4*(1), 1–15.

Ohkawa, H., Ohishi, N., & Yagi, K. (1979). Assay for lipid peroxides in animal tissues by thiobarbituric acid reaction. *Analytical Biochemistry*, *95*(2), 351–358.

Ortuño-Lizarán, I., Esquiva, G., Beach, T. G., Serrano, G. E., Adler, C. H., Lax, P., & Cuenca, N. (2018). Degeneration of human photosensitive retinal ganglion cells may explain sleep and circadian rhythms disorders in Parkinson's disease. *Acta Neuropathologica Communications*, *6*, 1–10.

Ortuño-Lizarán, I., Beach, T. G., Serrano, G. E., Walker, D. G., Adler, C. H., & Cuenca, N. (2018). Phosphorylated α-synuclein in the retina is a biomarker of Parkinson's disease pathology severity. *Movement Disorders*, *33*(8), 1315–1324.

Ortuño-Lizarán, I., Sánchez-Sáez, X., Lax, P., Serrano, G. E., Beach, T. G., Adler, C. H., & Cuenca, N. (2020). Dopaminergic retinal cell loss and visual dysfunction in

Parkinson disease. *Annals of Neurology*, *88*(5), 893–906.

Paleologou, K. E., Oueslati, A., Shakked, G., Rospigliosi, C. C., Kim, H.-Y., Lamberto, G. R., Fernandez, C. O., Schmid, A., Chegini, F., & Gai, W. P. (2010). Phosphorylation at S87 is enhanced in synucleinopathies, inhibits α-synuclein oligomerization, and influences synuclein-membrane interactions. *Journal of Neuroscience*, *30*(9), 3184–3198.

Poewe, W., Seppi, K., Tanner, C. M., Halliday, G. M., Brundin, P., Volkmann, J., Schrag, A.-E., & Lang, A. E. (2017). Parkinson disease. *Nature Reviews Disease Primers*, *3*(1), 1–21.

Rascunà, C., Russo, A., Terravecchia, C., Castellino, N., Avitabile, T., Bonfiglio, V., Fallico, M., Chisari, C. G., Cicero, C. E., & Grillo, M. (2020). Retinal thickness and microvascular pattern in early Parkinson's disease. *Frontiers in Neurology*, *11*, 533375.

Rausch, W.-D., Wang, F., & Radad, K. (2022). From the tyrosine hydroxylase hypothesis of Parkinson's disease to modern strategies: A short historical overview. *Journal of Neural Transmission*, *129*(5–6), 487–495.

Sadikan, M. Z., Nasir, N. A. A., Iezhitsa, I., & Agarwal, R. (2022). Antioxidant and anti-apoptotic effects of tocotrienol-rich fraction against streptozotocin-induced diabetic retinopathy in rats. *Biomedicine & Pharmacotherapy*, *153*, 113533.

Safadi, R. A., Musleh, A. S., Al-Khateeb, T. H., & Hamasha, A. A.-H. (2010). Analysis of immunohistochemical expression of k19 in oral epithelial dysplasia and oral squamous cell carcinoma using color deconvolution-image analysis method. *Head and Neck Pathology*, *4*, 282–289.

Smith, W. W., Margolis, R. L., Li, X., Troncoso, J. C., Lee, M. K., Dawson, V. L., Dawson, T. M., Iwatsubo, T., & Ross, C. A. (2005). α-Synuclein phosphorylation enhances eosinophilic cytoplasmic inclusion formation in SH-SY5Y cells. *Journal of Neuroscience*, *25*(23), 5544–5552.

Stefanis, L., Emmanouilidou, E., Pantazopoulou, M., Kirik, D., Vekrellis, K., & Tofaris, G. K. (2019). How is alpha-synuclein cleared from the cell? *Journal of Neurochemistry*, *150*(5), 577–590.

Sugeno, N., Takeda, A., Hasegawa, T., Kobayashi, M., Kikuchi, A., Mori, F., Wakabayashi, K., & Itoyama, Y. (2008). Serine 129 phosphorylation of α-synuclein induces unfolded protein response-mediated cell death. *Journal of Biological Chemistry*, *283*(34), 23179–23188.

Tatton, W. G., Kwan, M. M., Verrier, M. C., Seniuk, N. A., & Theriault, E. (1990). MPTP

produces reversible disappearance of tyrosine hydroxylase-containing retinal amacrine cells. *Brain Research*, *527*(1), 21–31.

Tenreiro, S., Eckermann, K., & Outeiro, T. F. (2014). Protein phosphorylation in neurodegeneration: friend or foe? *Frontiers in Molecular Neuroscience*, *7*, 42.

Tietze, F. (1969). Enzymic method for quantitative determination of nanogram amounts of total and oxidized glutathione: applications to mammalian blood and other tissues. *Analytical Biochemistry*, *27*(3), 502–522.

Tokuda, K., Baron, B., Kuramitsu, Y., Kitagawa, T., Tokuda, N., Morishige, N., Kobayashi, M., Kimura, K., Nakamura, K., & Sonoda, K.-H. (2018). Optimization of fixative solution for retinal morphology: a comparison with Davidson's fixative and other fixation solutions. *Japanese Journal of Ophthalmology*, *62*(4), 481–490.

Umeno, A., Biju, V., & Yoshida, Y. (2017). In vivo ROS production and use of oxidative stress-derived biomarkers to detect the onset of diseases such as Alzheimer's disease, Parkinson's disease, and diabetes. *Free Radical Research*, *51*(4), 413–427.

Varghese, F., Bukhari, A. B., Malhotra, R., & De, A. (2014). IHC Profiler: an open source plugin for the quantitative evaluation and automated scoring of immunohistochemistry images of human tissue samples. *PloS One*, *9*(5), e96801.

Xiong, N., Xiong, J., Jia, M., Liu, L., Zhang, X., Chen, Z., Huang, J., Zhang, Z., Hou, L., & Luo, Z. (2013). The role of autophagy in Parkinson's disease: rotenone-based modeling. *Behavioral and Brain Functions*, *9*(1), 1–12.

Zhou, Z., Chen, T., Wang, M., Jin, L., Zhao, Y., Chen, S., Wang, C., Zhang, G., Wang, Q., & Deng, Q. (2017). Pilot study of a novel classroom designed to prevent myopia by increasing children's exposure to outdoor light. *PLoS One*, *12*(7), e0181772.